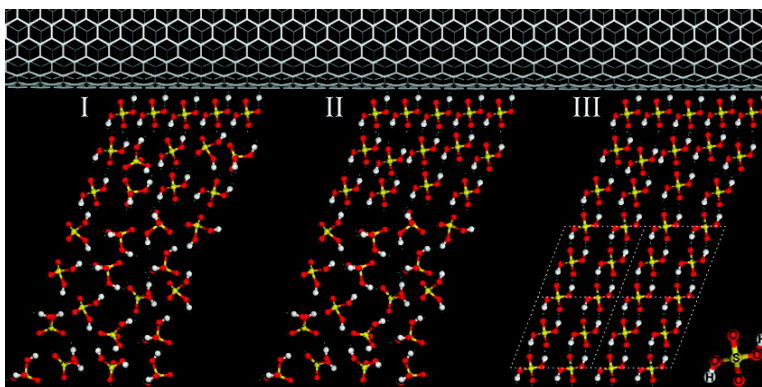


Single-Walled Carbon Nanotube-Templated Crystallization of HSO: Direct Evidence for Protonation

Wei Zhou, Paul A. Heiney, Hua Fan, Richard E. Smalley, and John E. Fischer

J. Am. Chem. Soc., **2005**, 127 (6), 1640-1641 • DOI: 10.1021/ja043131z • Publication Date (Web): 22 January 2005

Downloaded from <http://pubs.acs.org> on March 24, 2009



More About This Article

Additional resources and features associated with this article are available within the HTML version:

- Supporting Information
- Links to the 7 articles that cite this article, as of the time of this article download
- Access to high resolution figures
- Links to articles and content related to this article
- Copyright permission to reproduce figures and/or text from this article

[View the Full Text HTML](#)

Single-Walled Carbon Nanotube-Templated Crystallization of H₂SO₄: Direct Evidence for Protonation

Wei Zhou,[†] Paul A. Heiney,[‡] Hua Fan,[§] Richard E. Smalley,[§] and John E. Fischer^{*†}

Department of Materials Science and Engineering and Department of Physics and Astronomy, University of Pennsylvania, Philadelphia, Pennsylvania 19104, and Center for Nanoscale Science and Technology, Rice University, Houston, Texas 77005

Received November 15, 2004; E-mail: fischer@seas.upenn.edu

Single-walled carbon nanotubes (SWNTs) are novel one-dimensional (1-D) materials. Dissolved in anhydrous sulfuric acid, they induce a partial *positional* order in the surrounding solvent molecules.^{1,2} Calorimetric and X-ray diffraction data indicate a new phase of H₂SO₄ molecules surrounding the tubes as cylindrical shells.² We show here that the SWNT/H₂SO₄ interaction also induces short-range *orientational* order³ which templates the crystallization of free acid with specific orientations.

It was proposed that direct protonation of SWNTs is responsible for the formation of acid layers and consequently the dissolution of nanotubes,⁴ but there is little direct evidence for this model. It is difficult to distinguish protonation from redox doping as in acid-treated SWNTs.^{5,6} Here we use variable-temperature X-ray scattering to study the crystallization of H₂SO₄ in the presence of SWNTs. The structured acid wrapped around SWNTs remains partly ordered while the free acid surrounding the structured acid crystallizes at low *T*. The crystallization is templated by nanotubes, resulting in specific molecular orientations with respect to SWNTs such that a hydrogen bond points at the tube surface. This observation provides the strongest evidence thus far for protonation of SWNTs by superacid.

We used nanotube fibers spun from HiPco SWNT¹ for X-ray scattering experiments. The tubes are well aligned along the fiber axis, with an orientation mosaic dispersion of 31.5°. About 25 dry nanotube fibers ~5 mm in length and ~40 μm in diameter were packed into 0.5 mm glass capillaries, carefully maintaining the fibers parallel to the axis of the capillary. Anhydrous 102% sulfuric acid (with 2 wt % excess SO₃) was then added, and the fibers quickly swelled by 30–60% in diameter.¹ Samples containing more acid than necessary to completely swell the fibers are referred to as “swollen fibers with excess free acid”. To clearly investigate the phase behavior of structured acid, we also prepared “swollen fibers without excess free acid” by aspirating the free acid out of the capillary after weeks of immersion. All sample preparations involving acid were carried out in a drybox, with only brief exposure to air when the capillaries were sealed off.

X-ray diffraction experiments were performed at the CMC-CAT 9-ID beamline of the Advanced Photon Source (Argonne National Laboratory) using a 2-D SMART 1500 CCD detector 30 cm from the sample and 13.0 keV X-rays with a 100 μm × 100 μm beam spot. Sample temperature was controlled by an open cycle Joule–Thompson cold stage (high-pressure Ar) and heater equipped with a Be cylindrical window.⁷ All samples were measured in transmission for 5 s at each temperature with the fiber axis perpendicular to the incident beam.

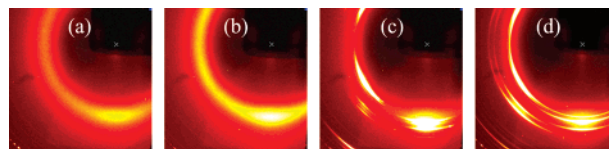


Figure 1. Two-dimensional detector images of X-ray scattering. (a) Swollen fiber without excess free acid at 300 K. The strong anisotropic scattering band centered at $\sim 1.5 \text{ \AA}^{-1}$ arises from the aligned acid associated with nanotubes. (b) Swollen fiber with excess free acid at 300 K. (c) Same sample as (b) but at 200 K. Preferred orientation of acid crystallites is obvious. The degree of alignment is the same as that of dry fiber, suggesting SWNT-templated crystallization. (d) Another swollen fiber sample contains more acid at 200 K, a small fraction of which is “truly free” and crystallizes randomly evidenced by the weak isotropic diffraction rings overlapping with anisotropic scattering. Note that for all samples, the fiber axis is in the horizontal direction (0° – 180°).

Figure 1a shows the detector image for a “swollen fiber without excess free acid” at 300 K. Acid molecules intercalate and dilate nanotube bundles in a disordered manner; thus, no Bragg diffraction from crystalline nanotube ropes⁸ was detected. The anisotropic scattering is solely from the structured acid associated with well-aligned nanotubes.² Upon cooling to 100 K or heating to 500 K (experimental limits), no change of the scattering pattern was observed, strongly suggesting that the acid associated with nanotubes remains partly ordered. This is consistent with our previous DSC results which show no signature of a phase transition between 170 and 300 K.² The high stability of the partly ordered acid phase implies that the association between nanotubes and the structured sulfuric acid is relatively strong. We cannot rule out the possibility of a glass transition.

Temperature-dependent X-ray scattering from the “swollen fiber with excess free acid” provides information on how the partly ordered acid affects the crystallization of excess free acid. Panels b and c of Figure 1 are detector images of one such sample at 300 and 200 K, respectively. Free acid crystallized at ~ 220 K upon cooling, and the crystallites show strong preferred orientation. The azimuthal mosaic full width at half-maximum (fwhm) of each peak is $\sim 33.1^\circ$, the same as that of dry fiber within experimental error. The fact that nanotube fibers and acid crystals have the same mosaic strongly indicates that the crystallization of acid is templated by nanotubes with a high degree of preferred orientation. In Figure 2, we show an enlarged version of Figure 1c with main diffraction indices labeled, and we plot the scattering profiles (intensity vs wave vector Q)⁹ obtained by azimuthal integration over 30° sectors centered at 210° , 225° , and 270° . The (2 0 0) and $(\bar{2} 0 2)$ Bragg peaks are centered about the direction perpendicular to the fiber axis, while (1 1 0), (0 0 2), and $(\bar{1} 1 1)$ Bragg diffractions are $\sim 30^\circ$ away from the fiber axis.¹⁰ This means that the (2 0 0) or $(\bar{2} 0 2)$ planes of the acid crystal are parallel to the nanotube axes with [0

[†] Department of Materials Science and Engineering, University of Pennsylvania.

[‡] Department of Physics and Astronomy, University of Pennsylvania.

[§] Rice University.

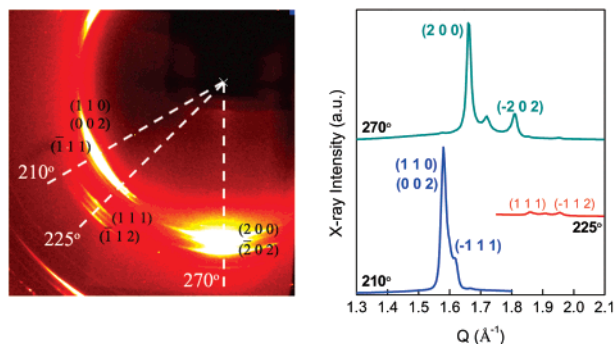


Figure 2. (Left) Enlarged version of Figure 1c with diffraction indices. (Right) Corresponding X-ray scattering profiles obtained by azimuthal integration of the 2-D data 30° wide in χ centered at 210° , 225° , and 270° .

1 0] direction normal to the nanotube axis. Due to the axial symmetry, the crystallites can assume any orientation about the nanotube axis and thus are polycrystalline within the plane normal to the nanotube axis. In other words, the only restriction is that either [0 0 1] or [1 0 1] direction must be parallel to the nanotube axis. Note that the (0 0 2) plane is not parallel to the tube axis; this is very important and will be addressed later. In Figure 1d, we show the detector image from another swollen fiber in a slightly larger capillary. Here, a small part of the excess acid is truly free, crystallizing as a more or less perfect powder and giving rise to the weak isotropic powder rings. The rest of the detector image mimics Figure 1c quite well. The reproducibility confirms that the templated crystallization effect is real.

Solid H_2SO_4 has a layered structure with hydrogen bonding only within (0 0 2) layers. Thus, if the (0 0 2) layer were parallel to the nanotube surface, the acid molecule would not be able to share a hydrogen bond with nanotubes. Both (2 0 0) and $(\bar{2} 0 2)$ surfaces are terminated with dangling hydrogen bonds. The fact that these planes are parallel to the nanotube axes, rather than the (0 0 2) plane of solid H_2SO_4 , strongly suggests that nanotubes are protonated by sulfuric acid. The ratio of integrated intensities of the (2 0 0) and $(\bar{2} 0 2)$ Bragg peaks is 3.44, slightly larger than 2.57 found¹⁰ in pure H_2SO_4 . This implies that there are slightly more crystals with (2 0 0) than with the $(\bar{2} 0 2)$ parallel to nanotube axis, which is reasonable since the molecular packing density in the (2 0 0) layers is ~ 1.1 times that in the $(\bar{2} 0 2)$ layers.

In Figure 3, we show schematically the SWNT-templated crystallization of H_2SO_4 through protonation interaction, implied by the data. We propose that the evolution from high temperature proceeds as follows. In the liquid phase (I), protonated nanotubes induce positional and orientational molecular order in the innermost layer of the structured acid. Molecules in the next two or three layers interact with the first layer via hydrogen bonding, acquiring weak positional and perhaps stronger orientational order and completing the semi-ordered region. Molecules more remote from the SWNT are bulklike. Upon cooling, molecules in the semi-ordered region become progressively more ordered in orientation while their positional order remains unchanged (II). Once the temperature reaches the critical point, the “free acid” crystallizes with crystallite orientations templated by the molecular orientations in the “structured acid” (III). In terms of positional order, the structured acid phase is also acting as a “buffer layer” for the crystal growth of free acid.

Although the concept of molecular ordering triggered by SWNTs was proposed previously for ionic liquids,¹¹ this is the first clear demonstration of SWNT-templated crystal growth. Considering the high curvature of the nanotube surface, SWNT-templated crystal

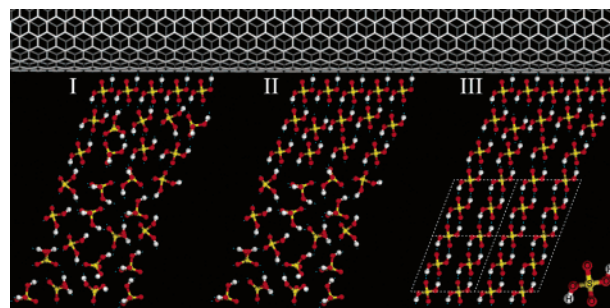


Figure 3. Schematic showing the crystallization of H_2SO_4 templated by SWNT or a rope. (I) Liquid phase of H_2SO_4 . Two or three layers of structured acid wrapped around nanotubes possess both positional order and orientational order, with the inside layer (negatively charged “ $\text{H}\cdots\text{HSO}_4^-$ ” which protonates SWNT) being most-ordered. Outside layers interact with the first layer via hydrogen bonding. Outside the two or three layers of semi-ordered acid is free bulk acid. (II) Molecular orientations in the semi-ordered region become ordered upon cooling with their positional order remaining unchanged. It represents a purely hypothetical but reasonable intermediate state. (III) Crystallization of “free acid” with its crystal orientation determined by the molecular orientation in the “structured acid”.

growth at molecular level is unexpected; presumably only when the interaction between the surrounding material and nanotube is strong enough is the templated crystal growth possible. Significant templated crystallization was not observed in other solvents (water, benzene) with immersed fibers. To compare SWNTs with graphite is also instructive. Graphite is less chemically active than nanotubes and thus cannot be protonated by superacid; only with the aid of electric potential can H_2SO_4 intercalate and dope graphite to form graphite intercalation compounds. Consequently, graphite is not expected to template the crystal growth of H_2SO_4 .

Acknowledgment. We thank D. M. Casa for his assistance with the X-ray measurements. This work was supported by ONR under the DURINT program, Grant N00014-01-1-0789 and by ONR N00014-03-1-0890 and by NSF Grant DMR-0102459. The Advanced Photon Source is supported by the U.S. Department of Energy under Contract No. W-31-109-ENG-38.

References

- Ericson, L. M.; Fan, H.; Peng, H.; Davis, V. A.; Zhou, W.; Sulpizio, J.; Wang, Y.; Booker, R.; Vavro, J.; Guthy, C.; Parra-Vasquez, A. N. G.; Kim, M. J.; Ramesh, S.; Saini, R. K.; Kittrell, C.; Lavin, G.; Schmidt, H.; Adams, W. W.; Billups, W. E.; Pasquali, M.; Hwang, W.; Hauge, R. H.; Fischer, J. E.; Smalley, R. E. *Science* **2004**, *305*, 1447–1450.
- Zhou, W.; Fischer, J. E.; Heiney, P. A.; Fan, H.; Davies, V. A.; Pasquali, M.; Smalley, R. E. *Phys. Rev. B: Condens. Matter* **2005**, in press.
- Krestov, G. A. *Thermodynamics of Solvation*; Ellis Horwood: Chichester, UK, 1991.
- Ramesh, S.; Ericson, L. M.; Davis, V. A.; Saini, R. K.; Kittrell, C.; Pasquali, M.; Billups, W. E.; Adams, W. W.; Hauge, R. H.; Smalley, R. E. *J. Phys. Chem. B* **2004**, *108*, 8794–8798.
- Sumanasekera, G. U.; Allen, J. L.; Fang, S. L.; Loper, A. L.; Rao, A. M.; Eklund, P. C. *J. Phys. Chem. B* **1999**, *103*, 4292–4297.
- Zhou, W.; Vavro, J.; Guthy, C.; Winey, K. I.; Fischer, J. E.; Ericson, L. M.; Ramesh, S.; Saini, R.; Davis, V. A.; Kittrell, C.; Pasquali, M.; Hauge, R. H.; Smalley, R. E. *J. Appl. Phys.* **2004**, *95*, 649–655.
- MMR Technologies, Inc., <http://www.mmr.com/xray.htm>.
- Thess, A.; Lee, R.; Nikolaev, P.; Dai, H.; Petit, P.; Robert, J.; Xu, C.; Lee, Y. H.; Kim, S. G.; Rinzler, A. G.; Colbert, D. T.; Scuseria, G. E.; Tomanek, D.; Fischer, J. E.; Smalley, R. E. *Science* **1996**, *273*, 483–487.
- Analyzed using Datasqueeze, <http://www.datasqueeze.com>.
- Solid H_2SO_4 has a monoclinic lattice, with parameters: $a = 8.14 \text{ \AA}$, $b = 4.70 \text{ \AA}$, $c = 8.54 \text{ \AA}$; $\beta = 111.42^\circ$ (Joint Committee on Powder Diffraction Standards file 83-2255). Interplanar angles between (2 0 0) and (1 1 0), (0 0 2), (1 1 1) are 68.6° , 58.2° , 70.5° , respectively, and those between (2 0 2) and the three planes are 71.8° , 57.7° , 55.7° , respectively.
- Fukushima, T.; Kosaka, A.; Ishimura, Y.; Yamamoto, T.; Takigawa, T.; Ishii, N.; Aida, T. *Science* **2003**, *300*, 2072–2074.

JA043131Z